



Synthesis of Peroxo-Titania with Enhanced Photocatalytic Activity and Stability Under Visible Light

S.Z. HU^{1,*}, F.Y. LI¹, Z.P. FAN¹ and J. ZHANG²

¹Institute of Eco-environmental Sciences, Liaoning Shihua University, Fushun 113001, P.R. China

²School of Petrochemical Engineering, Liaoning Shihua University, Fushun 113001, P.R. China

*Corresponding author: Tel: +86 24 23847473; E-mail: hushaozheng001@163.com

(Received: 7 January 2013;

Accepted: 18 September 2013)

AJC-14138

The peroxo-titania was prepared by H₂O₂ modification *in situ*. X-Ray diffraction, N₂ adsorption, UV-visible spectroscopy, FT-IR spectroscopy and X-ray photoelectron spectroscopy were used to characterize the prepared TiO₂ samples. The results indicated that the band gap did not decrease by modification, but formed surface complexes which could absorb visible light. The thermal decomposition of peroxo titanate complex cause the generation of oxygen *in situ*, which can hinder the oxygen vacancy formation and retains the strength of Ti-O-Ti network, thus stabilize the anatase phase and slow crystallite growth at high temperature. The obtained catalyst exhibited outstanding photocatalytic activity and stability under visible light. The possible mechanism was proposed.

Key Words: Peroxo-titania, H₂O₂, Photocatalyst, Phase transfer, Stability.

INTRODUCTION

The widespread applications of titanium dioxide in comparison to other semiconductor nanoparticles arise from the high redox potential, chemical stability, inexpensiveness and non-toxicity^{1,2}. Among the three polymorphs of titania, anatase phase is reported as the most photocatalytically active because of its higher charge-carrier mobility and an increased density of surface hydroxyls^{3,4}. On the other hand, rutile phase is found to be less active and photocatalytic activity, whereas brookite phase is seldom investigated⁵. Besides the influence of crystal structure, photocatalytic activity of titania depends on various factors such as phase purity, surface area, crystallite size, quantity and nature of dopants, method of preparation and the anatase/rutile ratio^{6,7}.

The most photocatalytically active anatase phase is metastable and irreversibly converted to the lesser photocatalytically active rutile at a temperature range of 600-700 °C. This limits the use of titania photocatalysts for the high temperature (≥ 800 °C) applications (*e.g.*, ceramic based building materials). Therefore, the improvement of anatase phase stability is one of the major challenges in ceramic industries^{8,9}.

It is known that titania has a wide band gap (3.2 eV), which confines its application to the UV region ($\lambda \leq 390$ nm). This means that the conventional photocatalysts can just utilize 5 % of the solar energy¹⁰. This has a significant impact on the commercial application of these materials. In order to utilize sunlight or artificial room light sources more effectively, the

development of visible light active titania is necessary. Therefore, many modification methods, including metal doping, nonmetal doping, co-doping and organic dye sensitization, have been investigated. Recently a new method, H₂O₂ modification has been reported by several research groups¹¹⁻¹³. Zou *et al.*¹², prepared H₂O₂-sensitizing TiO₂/SiO₂ composite photocatalysts. They found the obtained composite photocatalyst could absorb visible light at wavelength below 550 nm, thus exhibited visible light activity. Zou *et al.*¹³ synthesized the sulfated TiO₂ sensitized with hydrogen peroxide. The degradation of methyl orange on sulfated TiO₂ under optimal calcining conditions was significantly faster than that on P25 under visible light. Ohno *et al.*¹¹ prepared visible light responsive titanium peroxide by impregnating TiO₂ in H₂O₂. The obtained catalyst showed photocatalytic epoxidation activity of 1-decene under visible light. To resolve the problems mentioned above, a novel method to synthesis peroxo-titania by H₂O₂ modification *in situ* was reported in this work. The obtained catalyst still retained anatase phase after 800 °C calcination. The prepared peroxo-titania exhibited outstanding photocatalytic activity and stability under visible light. The possible mechanism was proposed.

EXPERIMENTAL

In a typical synthesis of peroxo-titania, 4 mL titanium tetrachloride was added to 100 mL cold water (0-5 °C) to form titanium oxychloride. Ammonia was added to above solution to adjust the pH value to 7. The obtained solid sample was

washed by deionized water to remove the chloride ions (tested by AgNO_3 solution). Then, the product was added into another solution contained 7.5 mL H_2O_2 and 100 mL deionized water and stirred for 1 h to form peroxy titanate complex. This solution was heated at 60 °C for 2 h to undergo gelation, then dried in oven at 80 °C for 20 h. The obtained xerogel was calcined at 450 °C for 2 h (5 °C/min). The obtained product was denoted as P1- TiO_2 , P0- TiO_2 , P2- TiO_2 and P3- TiO_2 were prepared by the same procedure above but addition of H_2O_2 0, 15 and 30 mL, respectively. For comparison, two more samples P0- TiO_2 -800 and P2- TiO_2 -800 were prepared following the same procedure as in the synthesis of P0- TiO_2 and P2- TiO_2 but calcined at 800 °C.

XRD patterns of the prepared TiO_2 samples were recorded on a Rigaku D/max-2400 instrument using $\text{CuK}\alpha$ radiation ($\lambda = 1.54 \text{ \AA}$). UV-visible spectroscopy measurement was carried out on a Jasco V-550 spectrophotometer, using BaSO_4 as the reference sample. The Brunauer-Emmett-Teller (BET)-specific surface areas (S_{BET}) of the samples were determined through nitrogen adsorption at 77 K (Micromeritics ASAP 2010). All the samples were degassed at 393 K before the measurement. Quantitative X-ray fluorescence analysis was performed by using an X-ray fluorescence spectrometer (SXF-1200 analyzer). XPS measurements were conducted on a Thermo Escalab 250 XPS system with $\text{AlK}\alpha$ radiation as the exciting source. The binding energies were calibrated by referencing the C 1s peak (284.6 eV) to reduce the sample charge effect.

Suspensions were prepared in deionised water by mixing TiO_2 catalyst with appropriate solutions of methylene blue. In a typical procedure, 0.1 g TiO_2 powders were dispersed in 100 mL solution of methylene blue (initial concentration $C_0 = 50 \text{ ppm}$) in an ultrasound generator for 10 min. The suspension was transferred into a self-designed glass reactor and stirred for 0.5 h in darkness to achieve the adsorption equilibrium. The concentration of methylene blue at this point was considered as the absorption equilibrium concentration C_0' . The adsorption capacity of a catalyst to methylene blue was defined by the adsorption amount of methylene blue on the photocatalyst ($C_0 - C_0'$). In the photoreaction under visible light irradiation, the suspension was exposed to a 110-W high-pressure sodium lamp with main emission in the range of 400-800 nm and air was bubbled at 130 mL/min through the solution. A cutoff filter was placed outside the water jacket to remove wavelengths below 420 nm to ensure irradiation completely by visible light. Additionally, irradiation at 450, 500 and 600 nm was carried out with a series of light filters. All runs were conducted at ambient pressure and 30 °C. At given time intervals, 4 mL suspension was taken and immediately centrifuged to separate the liquid samples from the solid catalyst. The concentrations of methylene blue before and after reaction were measured by means of a UV-visible spectrophotometer at a wavelength of 665 nm. It is the linear relationship between absorbance and concentration of liquid sample in the experimental concentration range. Therefore, the percentage of degradation $D \%$ was determined by the absorbances of the liquid sample before and after degradation.

RESULTS AND DISCUSSION

Fig. 1 shows the FT-IR spectra of P2- TiO_2 before and after calcination. Four bands were observed in the spectra of

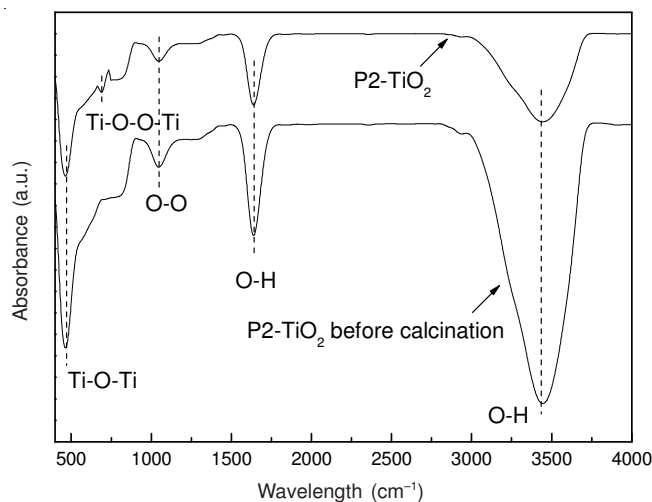
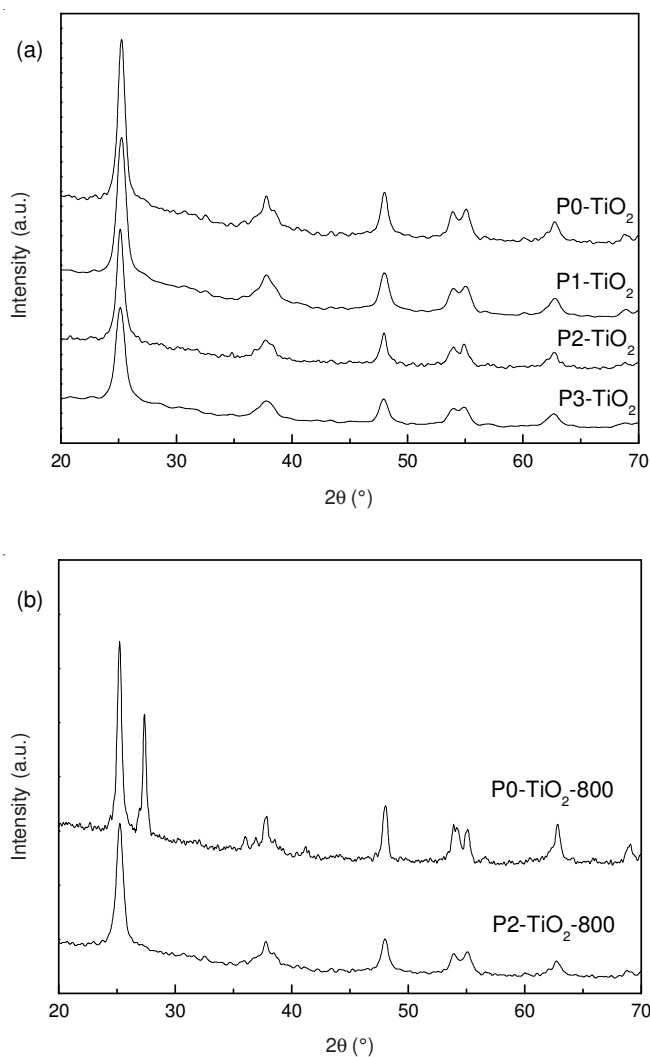


Fig. 1. FT-IR spectra of P2- TiO_2 before and after calcination

both samples. The bands at around 1640 and 3400 cm^{-1} are attributed to the bending and stretching vibrations of hydroxyl groups, respectively¹⁴. The band at 500 cm^{-1} is attributed to the O-Ti-O structure of TiO_2 . The band around 1040 cm^{-1} should be attributed to the O-O band¹⁵. After calcination, a new band around 690 cm^{-1} was observed. According to the previous reports, this band should be attributed to the Ti- μ -peroxide structure (Ti-O-O-Ti)^{16,17}. It is proposed that the calcination of peroxy titanate complex will cause the release of oxygen *in situ*. Such oxygen atom could insert the Ti-O lattice and form Ti-O-O-Ti structure.

The XRD patterns of prepared TiO_2 catalysts are shown in Fig. 2. All the samples were anatase phase (Fig. 2a). There was no observable structural difference between P0- TiO_2 and peroxy-titania. However, it is noted that the peak intensity decreased with the increase of H_2O_2 amount. The particle sizes of the samples were calculated by their XRD patterns according to the Debye-Scherrer equation. The results showed that the particle size decreased obviously (35, 31, 27 and 24 nm for P0- TiO_2 , P1- TiO_2 , P2- TiO_2 and P3- TiO_2). In Fig. 2b, the mix phase of anatase and rutile was observed for P0- TiO_2 -800, indicating partial TiO_2 sample was transferred from anatase phase to rutile phase under high temperature. However, for P2- TiO_2 -800, pure anatase phase was observed. Besides, according to the Debye-Scherrer equation, the particle size of P2- TiO_2 -800 was 28 nm, smaller than that of P0- TiO_2 -800 (39 nm). Therefore, it is deduced that the formation of peroxy-titania slowed crystallite growth and restrained the phase transfer. Generally speaking, the process of anatase to rutile phase transformation involves breaking of only two of the six Ti-O bonds in anatase¹⁸. This usually commences with oxygen vacancy formation, which accelerates the Ti-O bond breaking and phase transition associated with crystallite growth. Under normal synthesis conditions, high temperature treatment of titania always results in the formation of oxygen vacancies¹⁹⁻²¹. During the high temperature treatment, the Ti-O-Ti network weakens and this facilitates the Ti-O bond breaking and a consequent structural rearrangement to a thermodynamically stable rutile phase¹⁸. In this investigation, the thermal decomposition of peroxy titanate complex cause the generation of oxygen *in situ*, which can hinder the oxygen vacancy formation and retains

Fig. 2. XRD patterns of prepared TiO₂ samples

the strength of Ti-O-Ti network, thus stabilize the anatase phase and slow crystallite growth. The lattice parameters of the catalysts were measured using (1 0 1) and (2 0 0) in anatase crystal planes by using equations²¹:

$$d_{(hkl)} = \frac{\lambda}{2 \sin \theta} \quad (1)$$

$$d_{(hkl)}^{-2} = h^2 a^{-2} + k^2 b^{-2} + l^2 c^{-2} \quad (2)$$

where $d_{(hkl)}$ is the distance between crystal planes of (h k l), λ is the X-ray wavelength, θ is the diffraction angle of crystal plane (h k l), h k l is the crystal index. The a, b and c are lattice parameters (in anatase form, $a = b \neq c$). The results shown in Table-1 indicated that the decrease in c/a ratio associated with an increase of the lattice parameter a was identified with an increase of H₂O₂ content. This is probably due to that calcination of titania in an oxygen rich atmosphere could form oxygen *in situ*, which bond with an O atom on the lattice site, forming a Ti-O-O-Ti bond²². This results in the slight outward movement of the neighbouring Ti atoms and a consequent increase in lattice parameters. The increase of lattice parameters with an increase of H₂O₂ concentration may be due to the formation of more oxygen *in situ* during the heat treatment.

TABLE-1
LATTICE PARAMETERS OF PREPARED TiO₂ SAMPLES

Catalyst	a (Å)	c (Å)	c/a
P0-TiO ₂	3.7703	9.4753	2.514
P1-TiO ₂	3.7737	9.4748	2.510
P2-TiO ₂	3.7769	9.4754	2.508
P3-TiO ₂	3.7811	9.4755	2.506

UV-visible spectra for prepared TiO₂ samples are shown in Fig. 3. It could be seen that no absorption in visible light region for the sample of P0-TiO₂ was observed. However, a tailing absorption in the visible region 400-700 nm were observed for prepared peroxo-titania samples. According to the previous report, this is due to the formation of a new intermediate between TiO₂ and H₂O₂¹³. This new intermediate should be the surface complexes resulting from the interaction between H₂O₂ molecule and valance-unfilled Ti(IV) of TiO₂ surface. Such absorption in the visible region should be assigned to the intramolecular ligand to metal charge-transfer transition within the surface titanium(IV)-hydrogen peroxide complexes. Moreover, the visible light absorption increased with increasing the H₂O₂ content. This is probably due to the formation of more surface complexes between H₂O₂ molecule and TiO₂. Besides, no shift of the absorption edge was observed for the peroxo-titania samples, indicating the band gap energy was not decreased.

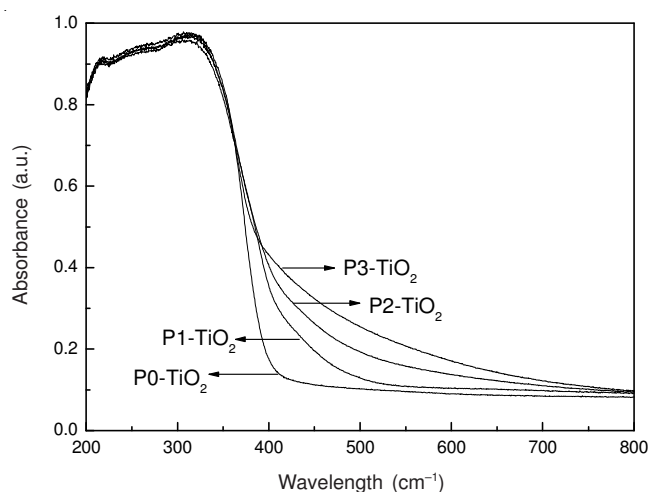
Fig. 3. UV-visible diffuse reflectance spectra of prepared TiO₂ samples

Fig. 4 shows the XP spectra of P0-TiO₂ and P2-TiO₂ in the region of Ti 2p (a) and O 1s (b). In the spectra of Ti 2p, the obvious shift to higher binding energy was observed for P2-TiO₂. This is probably due to that oxygen atom insert the Ti-O lattice to form Ti-O-O-Ti structure, which change the chemical environment of Ti. Due to the higher electronegativity of oxygen, more electrons may be transferred from Ti to O, leading to the decreased electron density on Ti atoms. It is known that a increase in binding energy implies the decrease of the electron density. Therefore, it is reasonable that the binding energy increased for P2-TiO₂. In Fig. 4b, the spectra of O 1s, the peak position did not shift for P2-TiO₂, whereas the peak intensity increased obviously. The O/Ti ratio of prepared TiO₂ samples was calculated and shown in Table-2. Modification of the titania precursors with H₂O₂ results in a significant increase

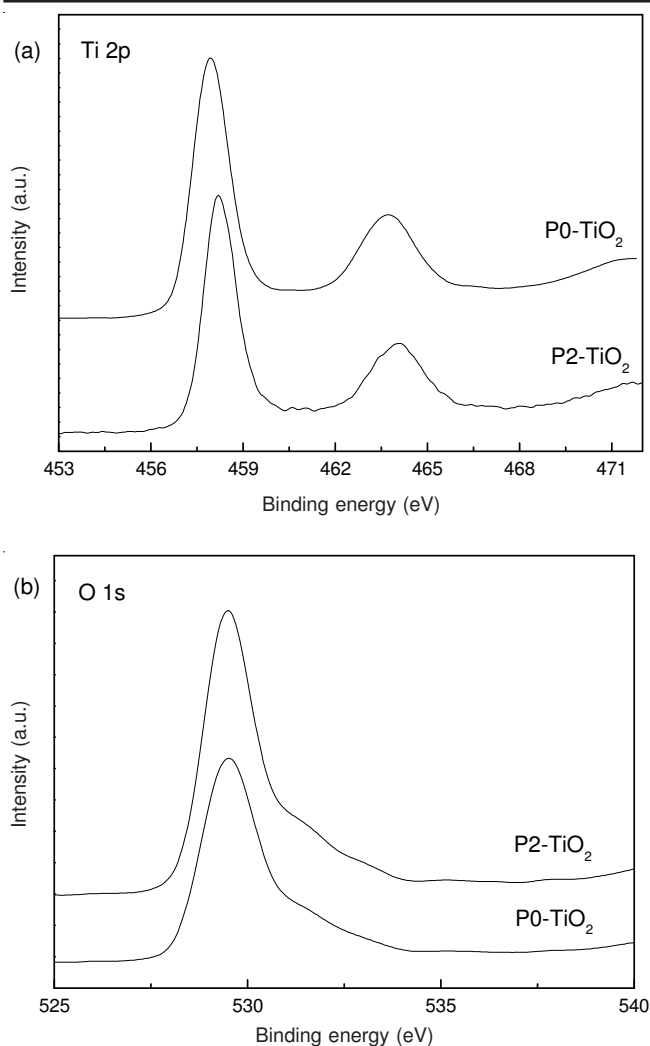


Fig. 4. XPS spectra of P0-TiO₂ and P2-TiO₂ in the region of Ti 2p (a), O 1s (b)

Catalyst	Ti 2p (at. %)	O 1s (at. %)	O/Ti
P0-TiO ₂	33.22	66.78	2.01
P1-TiO ₂	32.89	67.11	2.04
P2-TiO ₂	32.68	67.32	2.06
P3-TiO ₂	32.47	67.53	2.08
P0-TiO ₂ -800	33.29	66.71	2.0
P2-TiO ₂ -800	32.95	67.05	2.03

in the oxygen content and O/Ti ratio of the titania samples. P3-TiO₂ exhibited the highest oxygen content and O/Ti ratio, 67.53 at. % and 2.08. For P2-TiO₂-800, the oxygen content and O/Ti ratio decreased compared with P2-TiO₂. This is probably due to that partial Ti-O-O-Ti structure was destroyed under such high temperature. Therefore, it is concluded from above results (O/Ti ratio, Ti 2p and O 1s binding energies, FT-IR and XRD results) that the peroxo-titania was formed by modification with H₂O₂.

The photocatalytic activities of prepared TiO₂ samples under visible light are shown in Fig. 5. P0-TiO₂ exhibited no activity, agreeing well with the result from the UV-visible analysis that P0-TiO₂ had no response to visible light. For the peroxo-titania samples, the photocatalytic activity increased obviously. P2-TiO₂ exhibited the highest methylene blue

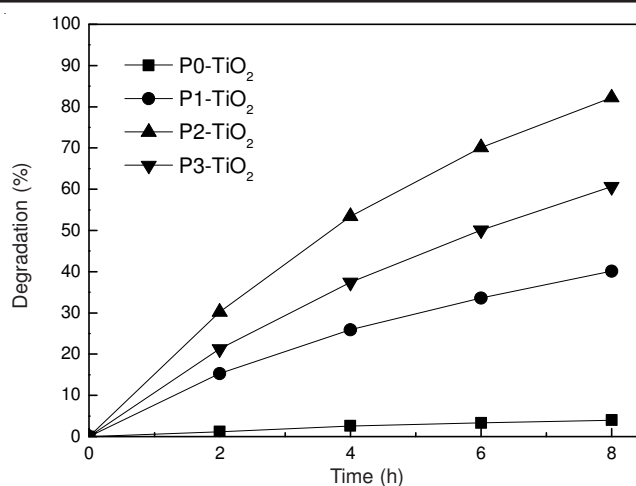


Fig. 5. Photocatalytic performances of prepared TiO₂ samples in the degradation methylene blue under visible light irradiation

conversion, over 80 % after 8 h. P3-TiO₂ with the highest oxygen content showed the much lower methylene blue conversion compared with P2-TiO₂ (60 % after 8 h). This is probably due to the difference in adsorption capacity of methylene blue. It is known that the S_{BET} strongly influences the adsorption capacity of the catalyst. In this investigation, the nitrogen adsorption results indicated that the S_{BET} of P0-TiO₂, P1-TiO₂, P2-TiO₂ and P3-TiO₂ was 63, 72, 88 and 93 m² g⁻¹, respectively. However, the adsorption capacity of methylene blue decreased in the order: P2-TiO₂ > P1-TiO₂ > P0-TiO₂ > P3-TiO₂, which was not consistent with the S_{BET} result completely. This should be due to the coverage of TiO₂ surface by excess surface complexes, leading to a decreased adsorption sites. Therefore, the methylene blue conversion of P3-TiO₂ was lower than that of P2-TiO₂.

Ohno *et al.*¹¹ prepared visible light responsive titanium peroxide by impregnating TiO₂ in H₂O₂. However, the obtained Ti-η²-peroxide structure is unstable. H₂O₂ need to be provided continuously during the photo-reaction to form the new Ti-η²-peroxide structure. To check the catalytic stability of prepared peroxo-titania catalyst, the photocatalytic performances of P2-TiO₂ were investigated in four cycles (not shown here). No decrease in activity was observed after four cycles, indicating that the peroxo-titania is stable under visible light irradiation.

It is known that, when the TiO₂ catalyst is excited by a photon with the energy beyond the band gap, an electron (e⁻)-hole (h⁺) pair is generated. The e⁻ and h⁺ may migrate to the surface of the photocatalyst particle. The photogenerated electrons in the conduction band and holes in the valence band of TiO₂ will react with O₂ and OH⁻, respectively to generate highly active •O₂⁻ and •OH species. Such highly active species are responsible for the decomposition of reactant^{1,2}. In order to clarify the photoreaction mechanism of peroxo-titania catalyst, in this investigation, *tert*-butyl alcohol (TBA, 10 mM) was added as •OH species scavenger. The result (not shown here) indicated that no obvious decrease in the photocatalytic activity of P2-TiO₂ was observed. It is deduced that the vis-activity should not be result from the •OH species. Therefore, h⁺ should not be formed during the photoreaction.

According to above result, the possible photoreaction mechanism should not the light excitation of TiO₂ but the

surface electron transfer from the surface complex to the TiO₂ conduction band. The possible mechanism of the photoinduced electron transfer and interface photoreaction of peroxo-titania catalyst was as follows. The TiO₂ catalyst can not be excited by visible light directly because the band gap energy did not decrease for the prepared peroxo-titania (Fig. 3). However, the calcination of peroxo titanate complex will cause the release of oxygen *in situ*, which insert the Ti-O crystal lattice and form surface complexes (Ti-O-O-Ti). Such surface complexes extend photoresponse to visible light and can be excited by visible light. The excited surface complex injects an electron to the conduction band of the semiconductor and generates the conduction band electron. Such e⁻ will react with O₂ to generate highly active [•]O₂⁻, which is responsible for the decomposition of methylene blue.

Conclusion

The peroxo-titania was prepared by H₂O₂ modification *in situ*. The thermal decomposition of peroxo titanate complex cause the generation of oxygen *in situ*, which can hinder the oxygen vacancy formation and retains the strength of Ti-O-Ti network, thus stabilize the anatase phase and slow crystallite growth. The surface complexes (Ti-O-O-Ti structure) was formed between H₂O₂ molecule and valance-unfilled Ti(IV) of TiO₂ surface, which could absorb the visible light. P2-TiO₂ exhibited the highest methylene blue conversion under visible light. The possible photoreaction mechanism should be not the light excitation of TiO₂ but the surface electron transfer from the surface complex to the TiO₂ conduction band.

ACKNOWLEDGEMENTS

This work was supported by National Natural Science Foundation of China (No. 41071317, 30972418), National Key

Technology R & D Programme of China (No. 2007BAC16B07, 2012ZX07505-001), the Natural Science Foundation of Liaoning Province (No. 20092080).

REFERENCES

1. P.V. Kamat, *Chem. Rev.*, **93**, 267 (1993).
2. M.R. Hoffmann, S.T. Martin, W. Choi and D.W. Bahnemann, *Chem. Rev.*, **95**, 69 (1995).
3. A.L. Linsebigler, G. Lu and Y.T. Yates, *Chem. Rev.*, **95**, 735 (1995).
4. M.A. Fox and M.T. Dulay, *Chem. Rev.*, **93**, 341 (1993).
5. T. Miyagi, M. Kamei, T. Mitsuhashi, T. Ishigaki and A. Yamazaki, *Chem. Phys. Lett.*, **390**, 399 (2004).
6. M. Toyoda, Y. Nanbu, Y. Nakazawa, M. Hirano and M. Inagaki, *Appl. Catal. B*, **49**, 227 (2004).
7. E. Beyers, P. Cool and E.F. Vansant, *J. Phys. Chem. B*, **109**, 10081 (2005).
8. M. Machida, W.K. Norimoto and T. Kimura, *J. Am. Ceram. Soc.*, **88**, 95 (2005).
9. A. Mills and S.K. Lee, *J. Photochem. Photobiol. A*, **182**, 181 (2006).
10. Y.Q. Wang, X.J. Yu and D.Z. Sun, *J. Hazard. Mater.*, **144**, 328 (2007).
11. T. Ohno, Y. Masaki, S. Hirayama and M. Matsumura, *J. Catal.*, **204**, 163 (2001).
12. J. Zou and J.C. Gao, *J. Hazard. Mater.*, **185**, 710 (2011).
13. J. Zou, J.C. Gao and Y. Wang, *J. Photochem. Photobiol. A*, **202**, 128 (2009).
14. S.K. Samantaray and K.M. Parida, *J. Mater. Sci.*, **38**, 1835 (2003).
15. T. Yoko, K. Kamiya and K. Tanaka, *J. Mater. Sci.*, **25**, 3922 (1990).
16. G. Munuera, A.R. González-Elipe, A. Fernández, P. Malet and J.P. Espinós, *J. Chem. Soc. Faraday Trans.*, **85**, 1279 (1989).
17. B.J. Evance, *Chem. Commun.*, 682 (1969).
18. R.D. Shannon, *Chem. Abstr.*, **63**, 2468 (1964).
19. G.R. Torres, T. Lindgren, J. Lu, C.G. Granqvist and S.E. Lindquist, *J. Phys. Chem. B*, **108**, 5995 (2004).
20. Y. Lida and S. Ozaki, *J. Am. Ceram. Soc.*, **44**, 120 (1961).
21. X.Z. Shen, Z.C. Liu, S.M. Xie and J. Guo, *J. Hazard. Mater.*, **162**, 1193 (2009).
22. S. Na-Phattalung, M.F. Smith, K. Kim, M.H. Du, S.H. Wei, S.B. Zhang and S. Limpijumong, *Phys. Rev. B: Condens. Matter.*, **73**, 125205 (2006).